MHD Thermally Radiating Flow through Two Parallel Vertical Plates Channel in the Presence of Chemical Reaction, Hall, Joule, and Cross-Diffusion Effects

OKUYADE IGHOROJE W. A.[1,*], IRHIAKUMA CHRIS T.[2]
[1]Department of Mathematics and Statistics,
Federal Polytechnic of Oil and Gas,
Bonny Island,
NIGERIA

[2]Department of Computer Science,
Federal Polytechnic of Oil and Gas,
Bonny Island,
NIGERIA

**Corresponding Author*

Abstract: - MHD thermally radiating flow through two parallel vertical plate channels in the presence of chemical reaction, Hall, Joule, and cross-diffusion effects are examined. The fluid is assumed chemically reactive, electrically conducting, magnetically susceptible, viscous, incompressible, and Newtonian; the plates are porous, electrically conductive, and heated to a high-temperature regime to generate thermal rays. The flow system is highly interactive such that cross/double diffusion effects are present. The governing partial differential equations are solved by the method of Modified Homotopy Perturbation. Expressions for the concentration, temperature, velocity, Nusselt number, Sherwood number, and Wall shear stress are obtained, computed, and presented graphically and tabularly. The analysis of results shows, amongst others, that an increase in the Hall Effects increases the main velocity and wall shear stress on both plates and causes fluctuations in the cross-velocity profiles.

Key-Words: - Chemical reaction, Cross-diffusion, Hall Effect, Homotopy perturbation, Joule heating, MHD, Radiation, Suction, Vertical plates channel, Viscous dissipation.

Received: June 13, 2024. Revised: September 18, 2024. Accepted: November 19, 2024. Published: December 31, 2024.

1 Introduction

Hall and Joule's effects have applications in science and engineering settings. They are relevant in heating and sensor devices. Specifically, the Hall Effect, which has great immunity to dust, dirt, mud, and water has applications in magnetometers used for measuring magnetic field strength and inspecting tubing/pipeline leakages; optical and electromagnetic sensing devices like rotating speed sensors (found in bicycle wheels, gear teeth, automotive speedometers, electronic ignition systems); fluid flow sensors; current sensors; pressure sensors; smartphones; global positioning systems; automotive ignition and fuel injection; hydraulic valves; low power thruster devices for propelling space crafts in orbits/farther space. Similarly, Joule/Ohmic/resistive heating, which results from the conversion of electricity into desirable and non-desirable heat effects, predominant in integrated circuits, has applications in many devices like laboratory water bathe for reactions at warm temperature, laboratory hot plates for reactions at high temperature, domestic immersion water heater, infra-red thermal image light bulbs, bulb filaments, magnified scanning, electron microscopes, electric radioactive space heater, incandescent light bulb filament, soldering iron, clothing iron, and the likes.

The interaction of electric and magnetic fields in a flow system results in many factors that influence the flow. By application, when a wire carrying alternating current is applied to a non-zero resistive plate/conductor a voltage difference is created between the ends of the conductor in the electric field. The electric field accelerates the charge carriers (electrons, ions, and holes) on the plate in the direction of the electric field to give kinetic energy. At collision with each other on the plate, the

charged particles are scattered/randomized. The randomized/scattering motions result in a thermal effect called Joule/Ohmic heating, which is limited by viscosity, electric conductivity, and fouling deposits on the conductor, causing the temperature of the conductor to rise. By this, electric energy is converted into thermal energy. Joule heating is characterized by the product of the magnetic field parameter and Brinkman number. Also, the varying alternating currents lead to the heating of the plate non-uniformly. The thermal motion arising from the Joule heating produces a dissipating force that works mechanically to heat the fluid as it passes the plate. The flow of heat from the plate through the fluid in the presence of gravity produces convective currents, which positively influence the motion and chemical reaction. Similarly, the heating of the plate to a high-temperature regime leads to the emission of thermal radiant rays. More so, when alternating electric currents are applied to a non-zero resistive conductor/plate, the conductivity of the material allows the currents to pass through. If the electric currents are transverse to the conductor, and the magnetic field is perpendicular to the currents, a voltage difference across an electrical conductor is generated. The voltage difference is termed the Hall Effect. In an ionized gas, it is very relevant when the gas density is low and the applied magnetic field force is high. Therefore, Hall Effects can be described as a measure of the mobility of the charge carriers (free electrons and holes), current density, or the Lorentz force effect on the charges in the electric current and is a function of the magnetic field.

Considering the roles of the Hall Effect and Joule heating in the fluid flow through two porous parallel plates vertical channel, [1] studied the Hall Effect in conducting fluids; [2] investigated the effects of Hall, thermal radiation, and chemical reaction on the flow; [3] studied the Hall effects on the transient flow of coupled-stressed fluids; [4] considered the Hall Effects on the oscillatory flow of a viscous fluid; [5] focused on the Hall effects on a transient convective flow with rotation; [6] investigated the Hall and inclined magnetic field effects on the flow when the system is rotating using finite difference approach. [7] examined the Hall, Joule, and thermal diffusion on the flow of couple-stressed fluid; [8] studied the Hall Effect, Joule heating, and Soret effects on the mixed convective flow using the Adomian Decomposition Method, and observed among others, that an increase in Hall Effect enhances the fluid concentration, velocity and the wall shear stress near the terminal plate, and the heat transfer rate at the initial plate but decreases the temperature, induced/cross velocity, the wall shear stress and mass transfer rate at the initial plate; increase in Joule heating increases the fluid temperature, concentration, main and cross velocities, heat and mass transfer at the terminal plate but decreases the heat and mass transfer at the initial plates. [9] studied the Hall effects on the transient impulsive flow with oscillatory pressure gradient and rotating channel; [10] studied the effect of thermal diffusion and inclined magnetic field on the mixed convective flow through a vertical parallel plates channel using the spectral quasi-linearization method and found that the inclined magnetic field amplifies the velocity but diminishes the temperature; the Hall Effect diminishes the velocity but increases the temperature; [11] researched on the Hall and ion-slip effects on couple-stressed fluid flow.

Neglecting the effects of Hall and Joule heating on the flow through parallel vertical plates channel, [12] studied numerically the MHD natural convective flow of a micro-polar fluid; [13] focused on the radiation effect in a hydro-magnetic Couette flow; [14] considered the effects of thermal radiation on the flow using the method of Homotopy Analysis; [15] examined the MHD oscillatory flow with periodic plate temperature; [16] focused on the heat source and Soret effects on the flow; [17] studied the chemical reaction effects on the MHD flow; [18] considered the effects of magnetic field and Brinkmann number on the mixed convective flow; [19] examined the Soret, Dufour and chemical reaction effects on the couple-stressed flow; [20] studied the transient flow of Maxwell fluid when the system is rotatory. [21] focused on the thermal effects on the MHD oscillatory flow with periodic plate temperature and viscous dissipation; [22] investigated the cross-diffusion effects on the non-Darcy free convective Power-law flow in the presence of stratification; [23] investigated the magnet-hydrodynamic mixed convective flow of nano-fluids; [24] investigated the Brinkmann and Hartmann parameters effects on the flow; [25] considered the hydro-dynamic natural convective flow of micro-polar fluid using differential transform.

Similarly, in the absence of a magnetic field, Hall and Joule heating effects, the flow through parallel vertical plates channel has been researched. For example, [26] investigated the flow when one of the plate is uniformly heated, and the other thermally insulated; [27] considered the effects of viscous dissipation and buoyancy; [28] examined the unsteady flow with heat flux at one boundary; [29] investigated the transient flow with

symmetrical heating; [30] studied the Couette–Poiseulli flow under forced convection; [31] considered the unsteady flow with asymmetrical heating/cooling walls; [32] studied the forced convective flow with viscous dissipation; [33] examined numerically the flow under low Prandtl number; [34] considered the fully developed free convective flow when the plates are asymmetrically heated with large temperature difference; [35] investigated the flow with constant temperature and mass diffusion; [36] studied the viscous dissipation and buoyancy effects in a laminar convective flow; [37] investigated the fully developed flow of micro-polar fluid; [38] investigated the mixed convective flow subject to Robin boundary conditions; [39] examined the radiation effects in a transient free convective flow using the Laplacian transform; [40] considered the effects of viscous dissipation and buoyancy in the presence of transpiration; [41] focused on the cross-diffusion effects on the flow of micro-polar flui using the Homotopy Analysis; [42] studied the heat analysis of micro-polar fluid flow, and [43] considered the heat transfer in a nano-particle flow, [44] investigated the unsteady natural convective flow with Newtonian heating.

[8] investigated the effects of Hall, Joule heating, and Soret on the mixed convective flow through two parallel porous vertical plate channels using the Adomian Decomposition approach. Their work has some deficiencies, hence this study. This work extends [8] to include the effects of thermal radiation, Dufour, and chemical reaction on the flow using the Modified Homotopy Perturbation approach.

In the sections below, the problem is formulated, solved, analyzed, discussed, and conclusions are drawn.

2 Problem Formulation

2.1 Physics of the Problem and Mathematical Formulation

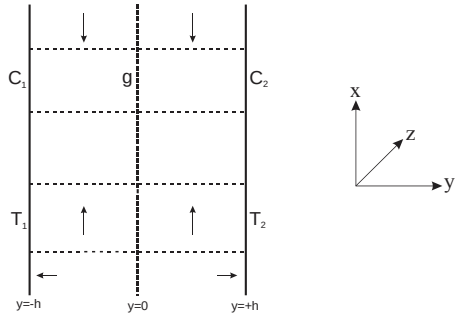

Fig. 1: A Physical Model of a Two Parallel Plates Vertical Channel

We consider the MHD thermally radiating flow through two parallel vertical plate channels in the presence of chemical reaction, Hall, Joule, and cross-diffusion effects. The schematic is shown in Figure 1. The plates are placed vertically upward in the x-direction and extend infinitely in the x- and z-axis, and perpendicular to the y-axis. Also, the plates are placed at $y=\pm h$ and $y=0$ as the centre of the channel. The model is developed based on the assumptions that the fluid is incompressible, viscous, Newtonian, chemically reacting, electrically conducting, magnetically susceptible, and optically thick. The plates are rectangular and porous and coated with some chemical substances to initiate a chemical reaction, heated electrically to produce the Joule heating effect, and to a degree of hotness to generate the thermal radiation effect. There are temperature and concentration differences, respectively between the equilibrium temperature and concentration of the fluid and those at the walls such that convection currents are generated. A transverse magnetic field is applied in the y-direction but with negligible induction effect assumed (for smallness when compared with the applied magnetic field) such that the magnetic Reynolds number becomes insignificant. The suctions/injections at the walls are constant. The pressure is along the x-axis, and $\partial p/\partial x$ is constant. The system is highly interactive such that the simultaneous effects of Dufour and Soret numbers are seen. An additional force is generated on the z-axis due to the Hall current, and this gives rise to a cross-flow, making the problem 3-dimensional. Buoyancy forces and uniform pressure gradient in the x-direction lead to mixed convection flow. Also, assuming fluid is injected into the channel through the lower wall and sucked through the upper wall with the same velocity V_0; at infinity, the flow is fully developed. Therefore, if (u,v,w) are the velocity (metre/sec) components in the (x,y,z) co-ordinates; u is the velocity in the x-axis and is along the plates; v is the constant suction at the walls and at the same time the velocity along the y-axis; w is the velocity along the z-axis, T and C are fluid temperature (Kelvin) and concentration (mol/cm^3), T_∞ and C_∞ are equilibrium temperature and concentration of the fluid, respectively. By the one-dimensional flow theory, the only independent variable is y (metre). Using Boussineq's approximation, the governing

equations of the mass balance, momenta, energy, and diffusion become.

$$\frac{\partial v}{\partial y}=0\Rightarrow v=v_o=constant \tag{1}$$

$$v_o\frac{\partial u}{\partial y}=u\frac{\partial^2 u}{\partial y^2}+g_xB_t(T-T_\infty)+g_xB_c(C-C_\infty)-\frac{\sigma_eB_o^2}{\rho}\frac{(u+mw)}{(1+m^2)}-\frac{\varepsilon u}{k}u-\frac{\partial p}{\partial x} \tag{2}$$

$$v_o\frac{\partial w}{\partial y}=u\frac{\partial^2 w}{\partial y^2}+\frac{\sigma_eB_o^2}{\rho\mu_m}\frac{(mu-w)}{(1+m^2)}-\frac{\varepsilon u}{k}w \tag{3}$$

$$v_o\frac{\partial T}{\partial y}=\frac{k}{\rho C_p}\frac{\partial^2 T}{\partial y^2}+\frac{\upsilon}{C_p}\left[\left(\frac{\partial u}{\partial y}\right)^2+\left(\frac{\partial w}{\partial y}\right)^2\right]+\frac{\sigma_eB_o^2(u^2+w^2)}{\rho C_p(1+m^2)}+\frac{Dk_T}{C_pC_s}\frac{\partial^2 C}{\partial y^2}-\frac{1}{\rho C_p}\frac{\partial q_r}{\partial y} \tag{4}$$

$$v_o\frac{\partial C}{\partial y}=D\frac{\partial^2 C}{\partial y^2}+\frac{Dk_T}{T_m}\frac{\partial^2 T}{\partial y^2}-k_r^2(C-C_\infty) \tag{5}$$

where g_x is the acceleration due to gravity; B_t and B_c are the volumetric expansion of the fluid due to temperature and concentration, respectively; C_p is the specific heat capacity (J/kgK) of the fluid at constant pressure; D is the mass diffusivity coefficient; k is the thermal diffusivity coefficient; k_T is the diffusivity ratio of the fluid; T_m is the mean temperature of the fluid; C_s is the concentration susceptibility of the fluid, k_r^2 is the chemical reaction rate term; ε is the porosity of the plate.

From the physical model, Figure 1, one plate is on the negative axis of the y-axis, and the other is on the positive axis. Taking y=0 as the centre/origin of the channel and from which the fluid flows towards and along with each plate, T_1 and C_1 are the temperature and concentration at the induced plate ($y=-h$), and T_2 and C_2 are the temperature and concentration at the terminal plate ($y=+h$).Then, the boundary conditions of the fluid become

$$u=0,w=0,T=T_1,C=C_1 \quad \text{at} \quad y=-h \tag{6}$$

$$u=0,w=0,T=T_2,C=C_2 \quad T=T_2,C=C_2 \quad \text{at} \quad y=+h \tag{7}$$

where h is the distance between the centre of the channel and the parallel plates.

Assuming the fluid is optically thick, adopting the Roseland approximation, we have:

$$q_r=-\frac{4\sigma}{3\alpha}\frac{\partial T^4}{\partial y} \tag{8}$$

where σ is Stefan-Boltzmann constant, α is the optical depth. Taking the temperature difference between the adjacent fluid layers to be small, and given that T^4 can be expressed in Taylor series expansion as a linear function about the ambient temperature T_∞, we get:

$$T^4=4T_\infty^3T-3T_\infty^3 \quad \text{([45], [46])} \tag{9}$$

By equation (9), we have:

$$\frac{\partial q_r}{\partial y}=-\frac{16\sigma T_\infty^3}{3\alpha}\frac{\partial^2 T}{\partial y^2} \tag{10}$$

(The higher-order term neglected), and equation (4) becomes:

$$v_o\frac{\partial T}{\partial y}=\frac{k}{\rho C_p}\frac{\partial^2 T}{\partial y^2}+\frac{\upsilon}{C_p}\left[\left(\frac{\partial u}{\partial y}\right)^2+\left(\frac{\partial w}{\partial y}\right)^2\right]+\frac{\sigma_eB_o^2(u^2+w^2)}{\rho C_p\mu_m(1+m^2)}+\frac{Dk_T}{C_pC_s}\frac{\partial^2 C}{\partial y^2}+\frac{16\sigma T_\infty^3}{3\rho C_p\alpha}\frac{\partial^2 T}{\partial y^2} \tag{11}$$

Introducing the following dimensionless quantities:

$$\eta=\frac{y}{h^2},u=\frac{u_oGr}{h^2}f.w=\frac{u_oGr}{h^2}g,$$

$$\Theta=\frac{T-T_1}{T_2-T_1},\Phi=\frac{C-C_1}{C_2-C_1},\ \Pr=\frac{\mu C_p}{k},Sc=\frac{\mu}{D},$$

$$Gr=\frac{g_xB_t(T_2-T_1)h^3}{\mu^2},Gc=\frac{g_xB_c(T_2-T_1)h^3}{\mu^2},$$

$$Sr=\frac{Dk_T(T_2-T_1)}{T_m(C_2-C_1)}, Dr=\frac{Dk_T(C_2-C_1)}{C_s,(T_2-T_1)},$$
$$Br=\frac{\mu u_0^2}{\kappa_f(T_2-T_1)}, Da=\frac{u_0 k}{h^2}, \delta=\frac{k_r^2}{D},$$
$$J=MBr, \mathrm{Re}=\frac{\rho u_o h}{\mu}, \quad \lambda=\frac{Gr}{\mathrm{Re}}, A=\frac{\partial p}{\partial x} \tag{12}$$

(where η is a similarity independent variable; u_0 is the characteristic (entrance) velocity; f is the main velocity in the $x-$ axis, g is the induced velocity in the z-axis; Θ and Φ are the dimensionless concentration and temperature, respectively; M is the Hartmann number; Da is the Darcy number, δ is the rate of chemical reaction; Pr is the Prandtl number; Sc is the Schmidt number; Br is the Brinkmann number; Ra is the Raleigh number; Sr is the Soret number; Dr is the Dufour number; Gr is the Grashof number due to temperature difference; Gc is the Grashof number due to concentration difference; N is the buoyancy ratio; and J is the dissipative force called Joule heating; Re is the Reynolds number; λ is the mixed convection parameter; A is the constant pressure gradient) into equations (1) - (7) and (11), we have

$$\frac{\partial f}{\partial \eta}=0 \tag{13}$$

$$f''-\mathrm{Re}f'-\left(\frac{M}{(1+m^2)}+\frac{\varepsilon}{Da}\right)f+\lambda(\Theta+N\Phi)-\frac{Mm}{(1+m^2)}g-A=0 \tag{14}$$

$$g''-\mathrm{Re}g'-\left(\frac{M}{(1+m^2)}+\frac{\varepsilon}{Da}\right)g+\frac{Mm}{(1+m^2)}f=0 \tag{15}$$

$$\Theta''-\left(\mathrm{RePr}+\frac{4}{3}Ra\right)\Theta'+BrGr^2(f'^2+g'^2)+\frac{JGr^2}{(1+m^2)}(f^2+g^2)+Dr\,\mathrm{Pr}\,\Phi''=0 \tag{16}$$

$$\Phi''-\mathrm{Re}Sc\,\Phi'-\delta\Phi+ScSr\,\Theta''=0 \tag{17}$$

with the boundary conditions:

$$f=0, g=0, \Theta=0, \Phi=0 \quad \text{at} \quad \eta=-1 \tag{18}$$

$$f=0, g=0, \Theta=1, \Phi=1 \quad \text{at} \quad \eta=+1 \tag{19}$$

Re-writing equations (14) - (17), we have:

$$f''=\mathrm{Re}f'+\gamma_1 f-\lambda(\Theta+N\Phi)+\gamma_2 g+A \tag{20}$$

$$g''=\mathrm{Re}g'+\gamma_1 g-\gamma_2 f \tag{21}$$

$$\Theta''=\gamma_3\Theta'-\gamma_4(f'^2+g'^2)-\gamma_5(f^2+g^2)-\gamma_6\Phi'' \tag{22}$$

$$\Phi''=\gamma_7\Phi'+\delta^2\Phi-\gamma_8\Theta'' \tag{23}$$

where

$$\gamma_1=\left(\frac{M}{(1+m^2)}+\frac{\varepsilon}{Da}\right) \quad \gamma_2=\frac{Mm}{(1+m^2)},$$
$$\gamma_3=\left(\mathrm{RePr}+\frac{4}{3}Ra\right) \quad \gamma_4=BrGr^2,$$
$$\gamma_5=\frac{JGr^2}{(1+m^2)}, \quad \gamma_6=Dr\,\mathrm{Pr},$$
$$\gamma_7=\mathrm{Re}Sc, \quad \gamma_8=ScSr$$

Furthermore, amongst other factors influencing the flow are the Nusselt number (Nu), Sherwood number (Sh) and Skin friction (C_f). These are prescribed in non-dimensionalized forms as:

$$Nu=-\Theta'\Big|_{\eta=\pm1} \tag{24}$$

$$Sh=-\Phi'\Big|_{\eta=\pm1} \tag{25}$$

$$\mathrm{Re}C_f=f'\Big|_{\eta=\pm1} \quad ([8]) \tag{26}$$

3 Problem Solution

3.1 Method of Solution

An examination of equations (20) - (22) depicts that they are coupled. To make them tractable, we seek the Modified Homotopy Perturbation Method of solution:

$$L(u)+N(u)-f(u)=0$$

Addressing these equations in the HPM form, we have:

$$(1-p)f''=p\begin{pmatrix}-f''+\mathrm{Re}\,f'+\gamma_1 f-\lambda(\Theta+N\Phi)\\+\gamma_2 g+A\end{pmatrix}$$

$$(1-p)g''=p(-g''+\mathrm{Re}g'+\gamma_1 g-\gamma_2 f)$$

$$(1-p)\Theta''=p\begin{pmatrix}-\Theta''+\gamma_3\Theta'-\gamma_4\left(f'^2+g'^2\right)\\-\gamma_5\left(f^2+g^2\right)-\gamma_6\Phi''\end{pmatrix}$$

$$(1-p)\Phi''=p(-\Phi''+\gamma_7\Phi'+\delta^2\Phi-\gamma_8\Theta'')$$

such that

$$f''=p(\mathrm{Re}f'+\gamma_1 f-\lambda(\Theta+N\Phi)+\gamma_2 g+A) \quad (27)$$

$$g''=p(\mathrm{Re}g'+\gamma_1 g-\gamma_2 f) \quad (28)$$

$$\Theta''=p\begin{pmatrix}\gamma_3\Theta'-\gamma_4\left(f'^2+g'^2\right)-\gamma_5\left(f^2+g^2\right)\\-\gamma_6\Phi''\end{pmatrix} \quad (29)$$

$$\Phi''=p(\gamma_7\Phi'+\delta^2\Phi-\gamma_8\Theta'') \quad (30)$$

Expanding the dependent variables in terms of p:

$$\left.\begin{aligned}f&=f_o+pf_1+p^2f_2+\ldots\\g&=g_o+pg_1+p^2g_2+\ldots\\\Theta&=\Theta_o+p\Theta_1+p^2\Theta_2+\ldots\\\Phi&=\Phi_o+p\Phi_1+p^2\Phi_2+\ldots\end{aligned}\right\} \quad (31)$$

where p<1. Substituting equation (31) into equations (27) - (30), (18) and (19), we have

$$(f_o''+pf_1''+p^2f_2''+.)=p\left\{\begin{aligned}&\mathrm{Re}(f_o'+pf_1'\\&+p^2f_2'+.)\\&+\gamma_1(f_o+pf_1\\&+p^2f_2+.)\\&-\lambda[(\Theta_o+p\Theta_1\\&+p^2\Theta_{2..})\\&+N(\Phi_o+p\Phi_1\\&+p^2\Phi_2+.)]\\&+\gamma_2(g_o+pg_1\\&+p^2g_2+\ldots)\\&+A\end{aligned}\right\}$$

$$(g_o''+pg_1''+p^2g_2''+\ldots)=p\left\{\begin{aligned}&\mathrm{Re}(g_o'+pg_1'\\&+p^2g_2'+\ldots)\\&+\gamma_1(g_o+pg_1\\&+p^2g_2+\ldots)\\&-\gamma_2(f_o+pf_1\\&+p^2f_2+\ldots)\end{aligned}\right\}$$

$$(\Theta_o''+p\Theta_1''+p^2\Theta_2''+\ldots)=p\left\{\begin{aligned}&\gamma_3(\Theta_o'+p\Theta_1'\\&+p^2\Theta_2'+\ldots)\\&-\gamma_4[(f_o'+pf_1'\\&+p^2f_2'+.)^2\\&+(g_o'+pg_1'\\&+p^2g_2'+\ldots)^2]\\&-\gamma_5[(f_o+pf_1\\&+p^2f_2+.)^2\\&+(g_o+pg_1\\&+p^2g_2+\ldots)^2]\\&-\gamma_6(\Phi_o''+p\Phi_1''\\&+p^2\Phi_2''+\ldots)\end{aligned}\right\}$$

$$(\Phi_o''+p\Phi_1''+p^2\Phi_2''+...)=p\begin{Bmatrix}\gamma_7[(\Phi_o'+p\Phi_1'\\+p^2\Phi_2'+.)]\\+\delta^2[(\Phi_o+p\Phi_1\\+p^2\Phi_2+.)]\\-\gamma_8(\Theta_o''+p\Theta_1''\\+p^2\Theta_2''+...)\end{Bmatrix}$$

Collecting the coefficients of the powers of p in each case, we have:

For the Zeroth Order

$$f_o''=0 \quad (32)$$

$$g_o''=0 \quad (33)$$

$$\Theta_o''=0 \quad (34)$$

$$\Phi_o''=0 \quad (35)$$

For the First Order

$$f_1''=\mathrm{Re}f_o'+\gamma_1 f_o-\lambda(\Theta_o+N\Phi_o)+\gamma_2 g_o+A \quad (36)$$

$$g_1''=\mathrm{Re}g_o'+\gamma_1 g_o-\gamma_2 f_o \quad (37)$$

$$\Theta_1''=\gamma_3\Theta_o'-\gamma_4(f_o'^2+g_o'^2)-\gamma_5(f_{o2}+g_{o2})-\gamma_6\Phi_o'' \quad (38)$$

$$\Phi_1''=\gamma_7\Phi_o'+\delta\Phi_o-\gamma_8\Theta_o'' \quad (39)$$

For the Second Order

$$f_2''=\mathrm{Re}f_1'+\gamma_1 f_1-\lambda(\Theta_1+N\Phi_1)+\gamma_2 g_1 \quad (40)$$

$$g_2''=\mathrm{Re}g_1'+\gamma_1 g_1-\gamma_2 f_1 \quad (41)$$

$$\Theta_2''=\gamma_3\Theta_1'-\gamma_4(2f_o'f_1'+2g_o'g_1')-\gamma_6\Phi_1'' \quad (42)$$

$$\Phi_2''=\gamma_7\Phi_1'+\delta\Phi_1-\gamma_8\Theta_1'' \quad (43)$$

with boundary conditions:

$$f_o=0, f_1=0, f_2=0,\quad g_o=0, g_1=0, g_2=0,\quad \Theta_o=0, \Theta_1=0, \Theta_2=0,\quad \Phi_o=0, \Phi_1=0, \Phi_2=0, \quad \text{at } \eta=-1 \quad (44)$$

$$f_o=0, f_1=0, f_2=0,\quad g_o=0, g_1=0, g_2=0,\quad \Theta_o=1, \Theta_1=0, \Theta_2=0,\quad \Phi_o=1, \Phi_1=0, \Phi_2=0, \quad \text{at } \eta=+1 \quad (45)$$

Equations (32) - (45) are solved using Mathematica 11.2. See the Appendices for the solutions.

3.2 Results and Discussion

The solutions are computed and presented graphically and tabularly. For constant values of $Dr=0.5, Sr=0.5, Da=0.3, N=0.5, Gr=Gc=1.0, J=3.0, Br=3.0, A=2.0, \varepsilon=1.0, p=0.1$ and varied values of $m, Ra, \delta, M, \mathrm{Pr}, Sc, \lambda$ and Re the Figure 2, Figure 3, Figure 4, Figure 5, Figure 6, Figure 7, Figure 8, Figure 9, Figure 10, Figure 11, Figure 12, Figure 13, Figure 14, Figure 15, Figure 16, Figure 17, Figure 18, Figure 19, Figure 20, Figure 21 and Figure 22, and Table 1 and Table 2 in Appendix were obtained.

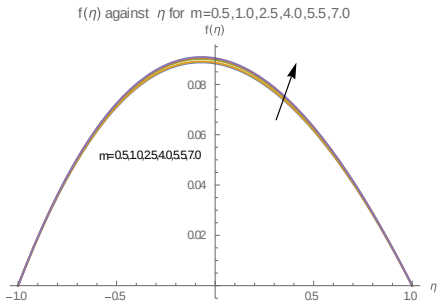

Fig. 2: Main Velocity-Hall Effect Profiles

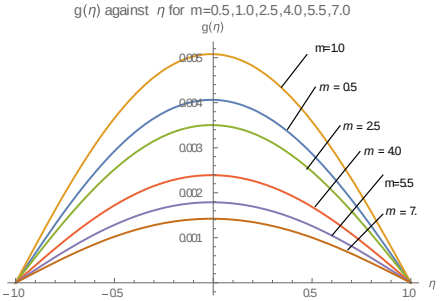

Fig. 3: Cross -Velocity-Hall Effect Profiles

The effects of the Hall currents on the flow are seen in Figure 2, Figure 3 and Table 1 (Appendix). Figure 2 shows that an increase in Hall currents increases the main velocity. Figure 3 depicts that an

increase in the Hall currents leads to fluctuations in the cross velocity. The cross velocity is highest at $m = 1.0$, drops for m=0.5, and decreases for $m \geq 2.5$. More so, Table 1 (Appendix) shows that the shear stress on the induced and terminal plates increases as the Hall current increases; the rate of heat and mass transfer at the induced and terminal plates is not affected by any increase in the magnitude of the Hall currents. When alternating electric currents are applied to a non-zero resistive conductor/plate, the conductivity of the material allows the currents to pass through. If the electric currents are transverse to the conductor, and the magnetic field is perpendicular to the currents, a voltage difference across the electrical conductor is generated. This voltage difference is the measure of the mobility of the charged carriers (free electrons and holes), current density, or the Lorentz force effect on the charges in the electric currents. More so, the mobility of the charged particles depends on the strength of the magnetic field, therein, the higher the magnetic field the higher the mobility of the charged particles, current density and Lorentz force. Therefore, an increase in the Hall Effects increases the interaction of the charged particles of the fluid, leading to an enhanced motion; as seen in Figure 2. This result aligns with [7] and [8]. Similarly, the fluctuation in cross velocity/velocity along the z-axis may be due to some other factors.

The effects of the Raleigh number on the flow are seen in Figure 4, Figure 5 and Figure 6. They show that an increase in the Raleigh number increases the main velocity, and mass volume/concentration, but decreases the temperature. Raleigh number is the product of thermal convection (Grashof number) and Prandtl number. It is associated with buoyancy driven-flow. When the walls of the plates are heated to a high-temperature regime, heat radiation or rays are released into the fluid. The depth of the penetration of the rays into the fluid depends on the fluid optical depth. The penetrated thermal rays in the fluid interact/energize its particles into wider space; thus accounting for what is seen in Figure 4. More so, energy is never lost but converted from one form to the other; the radiant rays/energy may be converted into light and refracted from the fluid. This may account for the drop in the fluid temperature structure seen in Figure 5. Additionally, when the thermal rays interact with the fluid particles, the particles are energized and spread into a wider space. In open systems, the fluid mass content escapes, thus leading to a loss or decrease in concentration; as seen in Figure 6.

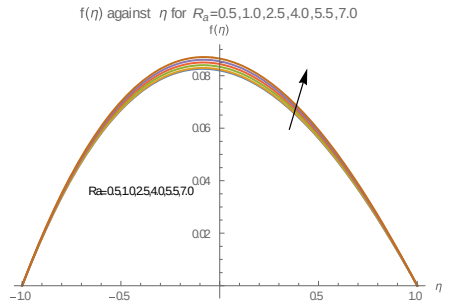

Fig. 4: Main Velocity-Raleigh Number Profiles

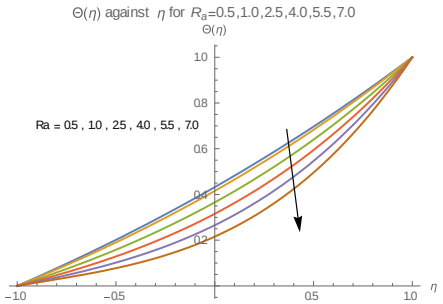

Fig. 5: Temperature-Raleigh Number Profiles

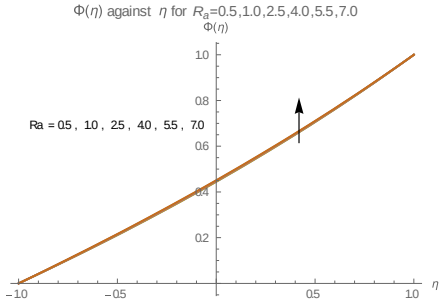

Fig. 6: Concentration-Raleigh Number Profiles

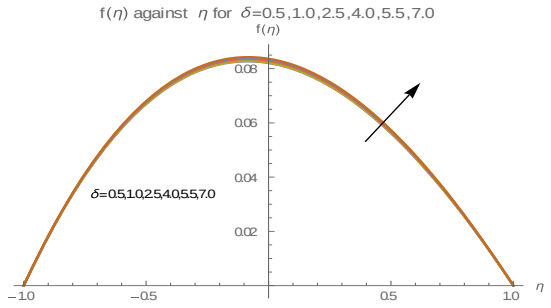

Fig. 7: Main Velocity-Chemical Reaction Rate Profiles

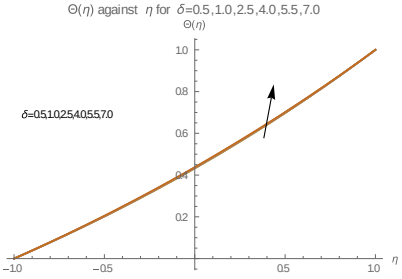

Fig. 8: Temperature-Chemical Reaction Rate Profiles

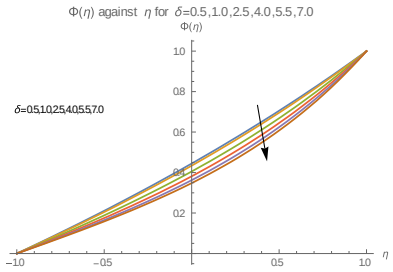

Fig. 9: Concentration-Chemical Reaction Rate Profiles

The effects of the rate of chemical reaction on the flow are seen in Figure 7, Figure 8, Figure 9 and Table 2 (Appendix). Figure 7, Figure 8, Figure 9 show that an increase in the rate of chemical reaction parameter increases the main velocity and temperature but decreases the mass volume. Also, Table 2 (Appendix) depicts that an increase in the chemical reaction rate parameter increases the shear stress near the induced and terminal plate wall; has no effect on the heat transfer rate at the induced plate but increases that at the terminal plate; increases the mass transfer rate at the induced plate but decreases that at the terminal plate. In a chemical reaction, the particles of the reacting materials interact. Their level of interaction amidst others depends on the nature and concentration of the reactants. The rate of interaction of the particles determines the velocity of the particles. This may account for the trends in Figure 7. Furthermore, energy is needed to form the new products in a chemical reaction. During a chemical reaction, heat is either absorbed (endothermic) or given out (exothermic). In the endothermic case, heat is absorbed. The effect of heat absorption tends to reduce the heat content of the reacting fluid particles. Similarly, in an exothermic reaction, heat is generated and released, possibly into the atmosphere. The released heat provides the energy for the bonding or formation of new products, and the heat energy released dampens the heat levels of the reacting particles. This accounts for what is seen in Figure 8. Additionally, in a chemical reaction, the content of any substance is used up to form new products. The rate at which new products are formed is a function of the rate of a chemical reaction. As the rate of the chemical reaction increases, new products are formed and the concentration of the reacting fluids/substances decreases, thus accounting for what is seen in the fluid concentration profiles, Figure 9.

The effects of the Hartmann number on the flow are seen in Figure 10 and Figure 11. They depict that an increase in the Hartmann number decreases the main velocity but increases the cross-velocity. In chemically reacting fluid, the fluid is either acidic or alkaline at different levels of strength. Upon this, their particles exist as charges or ions such that they conduct electricity. In the presence of a transverse magnetic field, they generate electric currents. The currents interact with a transverse magnetic field to generate a mechanical force (Lorentz force, a resisting force leading to friction on the fluid layers), which has the potency to freeze up fluid velocity. This accounts for profiles in Figure 10. Based on the known effect of Lorentz force on fluid velocity, the increase in the cross velocity may be due to some other factors.

The effects of the Prandtl number on the flow are seen in Figure 12, Figure 13 and Figure 14. They show that an increase in the Prandtl number increases the main velocity; decreases the temperature, and increases the mass volume.

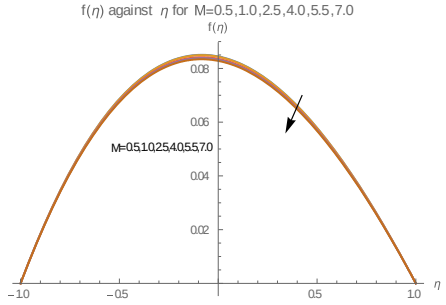

Fig. 10: Terminal Velocity-Hartmann Number Profiles

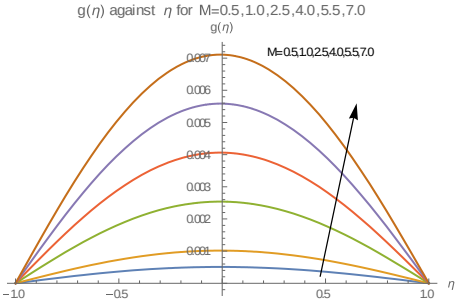

Fig. 11: Cross velocity-Hartmann Number Profiles

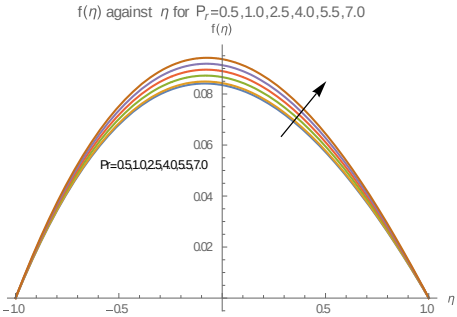

Fig. 12: Main Velocity-Prandtl Number Profiles

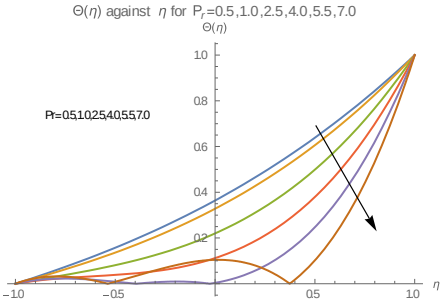

Fig. 13: Temperature-Prandtl Number Profiles

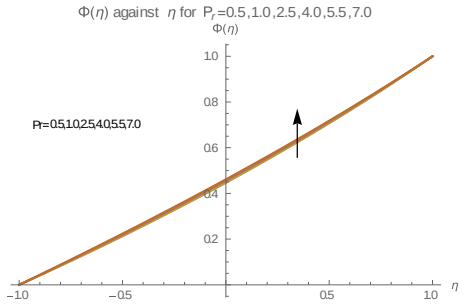

Fig. 14: Concentration-Prandtl Number Profiles

The Prandtl number of a fluid portrays the interaction relationship between material kinematic viscosity/momentum diffusivity and its thermal diffusivity. Its magnitude depends reciprocally on the interacting factors. Heat diffuses faster in a medium when its Prandtl number is small ($Pr<<1.0$). Prandtl number value rises when the thermal conductivity of the material/medium is smaller than its kinematic viscosity, and vice versa. By implication, an increase in the Prandtl number value shows that the material conductivity/diffusivity coefficient is small compared to the kinematic viscosity. As the grip on fluid particles is viscosity-based, higher kinematic viscosity/momentum diffusivity would mean higher interaction and, hence higher velocity. This accounts for what is seen in Figure 12. Similarly, the temperature of a system increases when there is a heat transfer from a source to the system through diffusion, and heat diffusion is a function of the thermal diffusivity coefficient. For the smallness of the thermal diffusivity coefficient the temperature is bound to decrease; thus accounting for the structure in Figure 13. Additionally, increasing Prandtl number values implies that the momentum diffusivity is higher, with higher momentum diffusivity the velocity increases. Upon this, concentration, being a function of velocity is bound to increase. This accounts for what is seen in Figure 14.

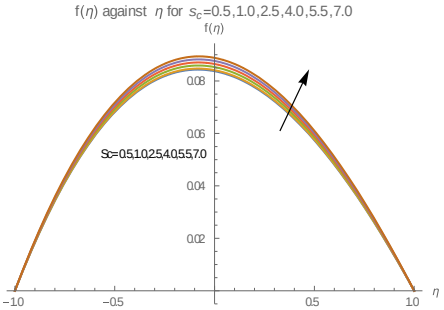

Fig. 15: Main Velocity-Schmidt Number Profiles.

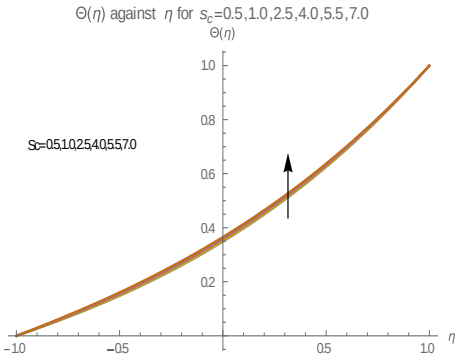

Fig. 16: Temperature-Schmidt Number Profiiles

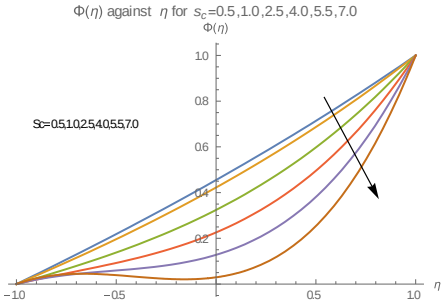

Fig. 17: Concentration-Schmidt Number Profiles

The effects of the Schmidt number are given in Figure 15, Figure 16 and Figure 17. They show that an increase in the Schmidt number increases the main velocity and temperature but decreases the concentration. Schmidt number arises from the interaction relationship between material kinematic viscosity/momentum diffusivity and its solutal diffusivity. Its magnitude is reciprocally dependent on the interacting factors. Mass diffuses faster in a medium when its Schmidt number is small ($Sc<<1.0$). Schmidt number value rises when the mass diffusivity of the material/medium is smaller than its kinematic viscosity, and vice versa. By implication, an increase in the Schmidt number value depicts that the material diffusivity coefficient is small compared to the kinematic viscosity. As the grip on fluid particles is viscosity-based, higher

kinematic viscosity/momentum diffusivity would mean higher interaction and, hence higher velocity. This accounts for what is seen in Figure 15. Additionally, increasing Schmidt number values implies that the momentum diffusivity is higher; hence the velocity is bound to increase. Upon this, temperature, as a function of velocity is bound to increase. This accounts for what is seen in Figure 16. Furthermore, the concentration of a system increases when there is a mass transfer from a source to the system by diffusion, which is a function of the solutal diffusivity coefficient of the fluid. For the smallness of the solutal diffusivity coefficient the concentration is bound to decrease; thus accounting for the structure in Figure 17.

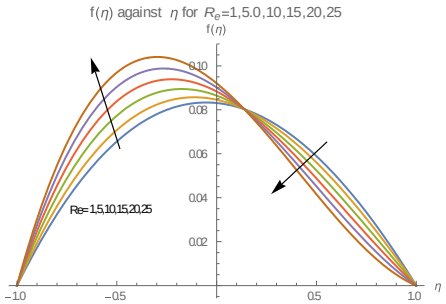

Fig. 18: Main Velocity-Reynolds Number Profiles

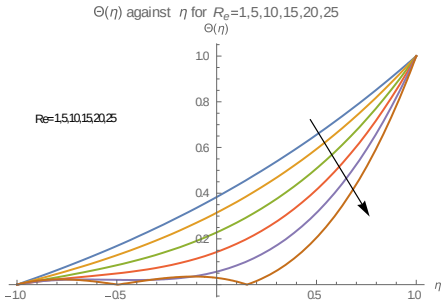

Fig. 19: Temperature-Reynolds Number Profiles

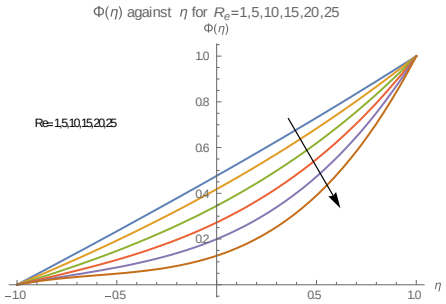

Fig. 20: Concentration-Reynolds Number Profiles

The effects of the Reynolds number on the flow are seen in Figure 18, Figure 19 and Figure 20. They show that an increase in Reynolds number increases the main velocity near the induced plate and a little bit towards the terminal plate, it develops a twist, then decreases; decreases the temperature and concentration. Reynolds number is known to enhance motion. Hence, the main velocity structure near the induced plate in Figure 18 aligns with this. Similarly, the decrease in velocity near the terminal plate, as in Figure 18 may be caused by some other factors. Furthermore, velocity, which is enhanced by the Reynolds number, is a function of energy/temperature and concentration. And as a function of velocity, the temperature and concentration are bound to increase. Therefore, the drop in the fluid temperature and concentration may be due to other factors.

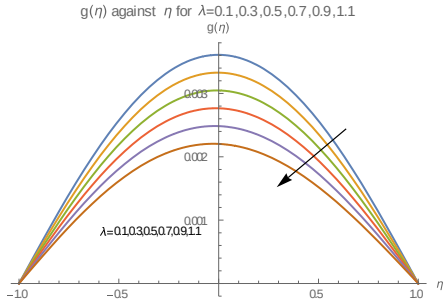

Fig. 21: Main Velocity-Mixed Convection Parameter Profiles

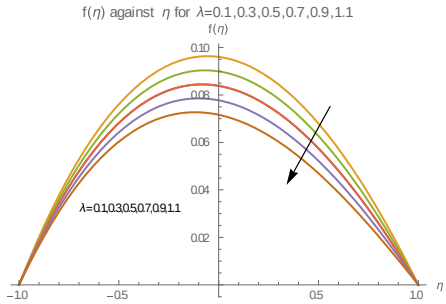

Fig. 22: Cross Velocity-Mixed Convection Parameter Profiles

The effects of the Mixed Convection parameter on the flow are seen in Figure 21 and Figure 22. They show that an increase in the Mixed Convection parameter decreases both the main and cross velocities. The mixed convection parameter arising from the interaction of the convective current resulting from the temperature differential between the external or temperature at the wall and the fluid ambient temperature compared with the momentum diffusivity (Reynolds number) has the potency for enhancing flow velocity due to its component factors. Therefore, the decrease in the velocities may be due to some other factors.

4 Conclusion

MHD thermally radiating flow through two parallel vertical channel plate channels in the presence of chemical reaction, Hall, Joule, and cross-diffusion effects is investigated. The analysis of the results shows that an increase in

- Hall Effects increase the main velocity, and wall shear stress on both plates; cause some fluctuations in the cross velocity, and have no effects on the rate of heat and mass transfer
- Rayleigh number increases the main velocity and temperature but decreases the concentration.
- Chemical Reaction Rate increases the main velocity, temperature, rate of heat transfer from the terminal plate, the rate of mass transfer from the induced plate, and wall shear stress on both the induced and terminal plates; decreases the concentration, and the mass transfer rate from the terminal plate.
- Hartmann number increases the cross velocity but decreases the main velocity
- Prandtl number increases the main velocity and concentration but decreases the temperature
- Schmidt number increases the main velocity and temperature but decreases the concentration
- Reynolds number increases the main velocity near the induced plate and a little bit towards the terminal plate, it develops a twist, then decreases; decreases the temperature and concentration.
- The mixed convection parameter decreases both main and cross velocities

Some of these results are benchmarked with those in the existing literature and are in good agreement.

References:

[1] I. Tani. Steady flow of conducting fluid in channels under transverse magnetic field with consideration of Hall effects, *Journal of Aerospace. Science*, Vol.29, 1962, pp. 297-305. https://doi.org/10.2514/8.9412.

[2] A. Manglesh, M.G. Gorla, MHD free convective flow through a porous medium in the presence of Hall current, radiation, and termal diffusion, *Indian Journal of Pure and Applied Mathematics,* 44, No.6, 2013, pp. 743-756. https://doi.org/10.1007/s13226-013-0040-9.

[3] G. Raju, M. Veera Krishna, R. Siva Prasad, Hall current effects on unsteady MHD three-dimensional flow of a couple stress fluid through a porous medium in a parallel plate channel, *International Journal of Physics and Mathematical Sciences,* Vol.3, No.1, 2013, pp. 18-31.

[4] B.P. Garg, K.D.Singh, A.K. Bansal, Hall current effect on visco-elastic (Walter's liquid model-B) MHD oscillatory convective channel flow through a porous medium with heat radiation. *Kragujevac Journal of Science,* Vol.36, 2014, pp. 19-32.

[5] M. Veera Krishna, J. Prakash, Hall current effects on unsteady MHD flow in a rotating parallel plate channel bounded by the porous bed on the Lower half - Darcy Lapwood model, *Open Journal of Fluid Dynamics,* Vol.5, 2015, pp. 275-294. http://dx.doi.org/10.4236/ojfd.2015.54029.

[6] R. Perven, M. Alam, Fluid flow through parallel plates in the presence Hall current and inclined magnetic field in a rotating system, *ASME Journal-2015 series,* Vol.84, No.1, 2015, pp. 49-68.

[7] K. Kaladhar, D. Srinivasacharya, Combined effects of Hall, Joule heating and thermal diffusion on a mixed convective flow in a vertical channel with couple stress fluid, *Frontiers in Heat and Mass Transfer,* Vol.7, No.6, 2016, pp. 11175-1186. https://doi.org/10.5098/hmt.7.6.

[8] C.H. Ram Reddy, K. Kaladhar, D. Srinavasacharya, T. Pradeepa, Influence of Soret, Hall and Joule heating effects on mixed convection flow saturated porous medium in a vertical channel by Adomian Decomposition Method, *De Gruyter Open Engineering Journal,* Vol.6, 2016, pp. 10-21. https://doi.org/10.1515/eng-2016-0003.

[9] C. Padma, S. Suneethra, Hall effects on MHD flow through a porous medium in a rotating parallel plate channel, *International Journal of Applied Engineering. Research,* Vol.13, No.11, 2018, pp. 9772-9789.

[10] K. Kaladhar, M. Reddy, D. Srinivasacharya, Inclined magnetic field and Soret effects on a mixed convective flow between vertical parallel plates, *Journal of Application, Analysis and Computing,* Vol.9, No.6, 2018, pp. 2111-2123. https://doi.org/10.11948/20180146.

[11] G.A.Shalaby, Couple stress and thermo-phoretic influence on free convective heat and mass transfer of viscoelastic fluid with

Hall and ion-slip effects, *Journal of Advances in Physics,* Vol.17, 2020, pp. 117-132. https://doi.org/10.24297/jap.v17i.8657.

[12] R. Bhargava, L. Kumar, H.S. Takhar, Numerical solution of the free convective flow of a micro-polar fluid between two parallel porous vertical plates, *International Journal of Engineering Science,* Vol.41, 2003, pp. 123-136. https://doi.org/10.1016/S0020-7225(02)00157-X.

[13] P. Mebine, Radiation effects on MHD Couette flow with heat transfer between two parallel plates. *Global Journal of Pure and Applied Mathematics,* Vol.3, No.2, 2007, pp. 191-202.

[14] S. Srinanvasacharya, R. Muthuraj, Effect of thermal radiation and space porosity on MHD mixed convective flow in a vertical channel using homology analysis method, *Communications in Non-Linear Sciences and Numerical Simulations*, Vol.15, No.8, 2010, pp. 2098-2108.

[15] N. Ahmed, K. Sarma, D.P. Barua, Magnetic field effect on the free convective oscillatory flow between vertical parallel plates with periodic plate temperature, *Journal of Applied Mathematical Sciences,* Vol.6, No.39, 2012, pp. 1913-1924.

[16] K. Chand, R. Kumar, S. Sharma, Hydromagnetic oscillating flow through a porous medium bounded by two vertical porous plates with heat source and Soret effects, *Advanced Applied Science Research,* Vol.3, No.4, 2012, pp. 2169-2178.

[17] R.N. Barik, Free convective heat and mass transfer in a vertical channel in the presence of chemical reaction, *International Journal of Analysis and Application,* Vol.2, No.2, 2013, pp. 151- 181. https://doi.org/10.1155/2013/297493.

[18] E. Salehi, R. Alizadeh, A. Darvish, The effects of MHD and Brinkman number on laminar mixed convection of Newtonian fluid between vertical parallel plates channel, *WSEAS Transaction on Heat and Mass Transfer,* Issue 4, Vol. 8, October 2013, p.139-145.

[19] D. Srinavasacharya, K. Kaladhar, Soret and Dufour effects on a free convective flow of a couple–stress fluid in a vertical channel with chemical reaction, *Chemical and Industrial Engineering Journal,* Q (19C1), 2013, pp. 45 -55. https://doi.org/10.2298/CICEQ111231041S.

[20] M. Veera Krishna, Md Irfan, Ahmed, Hall effects of unsteady MHD flow of Maxwell fluid through a porous medium in rotating parallel plate channel. *International Journal of Applied Mathematics and Engineering Sciences,* Vol.8, No.1, 2014, pp. 11-27.

[21] D. Sarma, N. Ahmed, P.K. Mahata, Effects of thermal radiation on the MHD free convective oscillatory flow between two vertical parallel plates with periodic plate temperature and dissipative heat, *Heat and Technology Journal,* Vol.32, No.(1-2), 2014, pp. 51-57.

[22] D. Srinavasacharya, J. Pranitha, C.H. Ram Reddy, A. Postelinicu, Soret and Dufour effects in non-Darcy free convection in a Power-law fluid in presence of magnetic field and stratification, *Heat Transfer Asian Research,* Vol.43, 2014, pp. 592-606.

[23] S. Das, R.N. Jana, O.D. Makinde, Mixed convective magneto-hydrodynamic flow in a vertical channel filled with nanofluids, *International Journal Engineering Science and Technology,* Vol.18, 2015, pp. 244-255. https://doi.org/10.1016/j.jestch.2014.12.009

[24] K.M. Joseph, P. Ayuba, A.S. Magaji, Effects of Brinkman number and magnetic field on laminar convection in a vertical plate channel, *Science World Journal,* Vol.12, No.4, 2017, pp. 58-62.

[25] J.C. Umavathi, A.J. Chamkhar, M. Shekar, Free convective flow of an electrically-conducting micro-polar fluid between two parallel porous plates using differential transform, *Journal of Applied Computation and Mechanics,* Vol.4, No.4, 2018, pp. 286-298. Doi:10.22055/JACM.2018.24272.1180.

[26] O. Miyatake, T. Fujii, H. Tanaka, Natural convection heat transfer between a vertical parallel plate with uniform heat flux and the other thermally insulated, *Heat Transfer-Japanese Research,* Vol.2, No.1, 1973, pp. 25-33.

[27] A. Barletta, Laminar convection in a vertical channel with viscous dissipation and buoyancy effects, *International Communication in Heat Mass Transfer,* Vol. 26, No.2, 1999, pp. 153-164. https://doi.org/10.1016/S0735-1933(99)00002-0.

[28] M. Narahari,S. Sreenadh, V.M. Soundagelkar, Transient free convective flow between a long parallel plates with constant heat flux at one boundary, *Journal of*

Thermo-Physics and Aeromechanics, Vol.9, No.2, 2002, pp. 287-293.

[29] B.K. Jha, A.K. Singh, H.S. Takdar, Transient free convective flow in a vertical channel due to symmetric heating, *International Journal of Applied Mechanics and Engineering,* Vol.8, No.3, 2003, pp. 497--502.

[30] S.H. Hashemabadi, Gh.S. Etemad, J. Thibault, Forced convection heat transfer of Couette-Poiseuilli flow of nonlinear visco-elastic fluids between parallel plates, *International Journal Heat and Mass Transfer,* Vol.47, 2004, pp. 3985-3991. https://doi.org/10.1016/j.ijheatmasstransfer.2004.03.026.

[31] A.K. Singh, T. Paul, Transient natural convection between two vertical walls heated/cooled asymmetrically, *International Journal of Applied Mechanics and Engineering,* Vol.11, No.1, 2006, pp. 143-154.

[32] O. Aydin, M. Avei, Laminar forced convection with viscous dissipation in a Couette-Poiseuilli flow between parallel plates, *Applied Energy,* Vol.83, 2006, pp. 856-867.

[33] A. Compo, O. Manca, B. Morrone, Numerical investigation of the natural convection flows for low-Prandtl fluids in vertical parallel-plates channels, *ASME Journal of Applied Mechanics,* Vol.73, 2006, pp. 96-107. https://doi.org/10.1115/1.1991867.

[34] A. Pantokratoras, Fully developed laminar free convection with variable thermo-physical properties between two open-ended vertical parallel plates heated asymmetrically with large temperature differences, *ASME Journal of Heat Transfer,* Vol.128, No.3, 2006, pp. 405-408. https://doi.org/10.1115/1.2175154.

[35] M. Narahari, Transient free convective flow between two long vertical parallel plates with constant temperature and mass diffusion, *Proceedings of World Congress on Engineering, London, U. K,* Vol.11, 2008.

[36] M. Narahari, Oscillatory plate temperature effects of free convection flow of dissipative fluid between long vertical parallel plates, *International Journal of Applied Mathematics and Mechanics,* Vol.5, No.3, 2009, pp. 30-46.

[37] S. Daniel, Y. Tella, J.K. Moses, Laminar convection in a vertical plate channel with viscous dissipation and buoyancy effects, *Journal of Mathematical Association of Nigeria (Abacus),* Vol.37, No.2, 2010, pp. 95-108.

[38] J.P. Kumar, J.C. Umavathi, A.J. Chamkhar, I. Pop, Fully-developed free convective flow of micro-polar fluid in a vertical channel, *Journal of Applied Mathematical Modeling,* Vol.34, 2010, pp. 1175-1186. https://doi.org/10.1016/j.apm.2009.08.007.

[39] F. Palnulescu, T.A. Gros, A.V. Lar, Mixed convection in a vertical channel subject to Robin boundary. *Studia University Babes, Bolyai Mathematica*, Vol.LV, No.2, 2010, 167-175.

[40] M. Narahari, Effects of thermal radiation and free convective currents on the unsteady Couette flow between two vertical parallel plates with constant heat flux at one boundary, *WSEAS Transaction on Heat and Mass Transfer*, Vol.5, No.1, 2010, pp. 21-30.

[41] A.S. Idowu, K.M. Joseph, C. Onwubuoya, W.D. Joseph, Viscous dissipation and buoyancy effects on laminar convection in a vertical channel with transpiration, *International Journal of Applied Mathematical Research,* Vol.14, 2013, pp. 456-463. https://doi.org/10.14419/ijamr.v2i4.1148.

[42] D. Srinivasacharya, S. Mekonnen, Flow of a micro-polar fluid between two parallel vertical plates with Soret and Duffour effects, *Arabian Journal of Science and Engineering,* Vol.39, 2014, pp. 5085-5093.

[43] A.T. Akinshil, J.O. Olofinkua, O. Olaye, Flow and heat transfer analysis of sodium alginate conveying copper nano-particles between two parallel plates, *Journal of Applied Computational Mechanical* Vol.3, 2017, pp. 258-266. https://doi.org/10.22055/jacm.2017.21514.1105.

[44] F. Zulkiflee, Q.A Muhammad, S. Shafie, A. Khan, Unsteady free convection flow between two vertical parallel plates with Newtonian heating, *Matematik,* Vol.35, No.2, 2019, pp. 117-27. https://doi.org/10.11113/matematika.v35.n2.1104.

[45] S.S. Shateyi, S.S. Motsa, P. Sibanda, The effects of thermal radiation, Hall currents Soret and Dufour on MHD flow by mixed convection over a vertical surface in porous media, *Mathematical Problems in Engineering,* 2010, pp. 1-20. https://doi.org/10.1155/2010/627475.

[46] W.I.A. Okuyade, T.M. Abbey, A.T. Gima-Laabel, Unsteady MHD free convective chemically reacting fluid flow over a vertical plate with thermal radiation, Dufour , Soret and constant suction effects, *Alexandria Engineering Journal,* Vol.57, 2018, pp. 3863-3871. https://doi.org/10.1016/j.aej.2018.02.006.

Contribution of Individual Authors to the Creation of a Scientific Article (Ghostwriting Policy)

The authors equally contributed in the present research, at all stages from the formulation of the problem to the final findings and solution.

Sources of Funding for Research Presented in a Scientific Article or Scientific Article Itself

No funding was received for conducting this study.

Conflict of Interest

The authors have no conflicts of interest to declare.

APPENDIX

$$f(\eta) = (0) + p[\frac{1}{4}(-2A + \lambda + \lambda N) + \frac{1}{12}\lambda(1+N)\eta$$
$$+\frac{1}{4}(2A - \lambda(1+N))\eta^2 - \frac{1}{12}(\lambda(1+N))\eta^3]$$
$$+p^2[\frac{1}{48}(10A\gamma_1 - 5\lambda(\gamma_1+\gamma_3+(\gamma_1+\gamma_7+\delta)N)$$
$$+\lambda(1+N)\mathrm{Re})$$
$$+\frac{1}{720}(-7\lambda(\gamma_1+(\gamma_1+\delta)N)$$
$$-60(-2A+\lambda+\lambda N)\mathrm{Re})\eta$$
$$+\frac{1}{24}(6A\gamma_1+3\lambda(\gamma_1+\gamma_3+(\gamma_1+\gamma_7+\delta)N)$$
$$-\lambda(1+N)\mathrm{Re})\eta^2$$
$$+\frac{1}{72}(\lambda(\gamma_1+(\gamma_1+\delta)N)$$
$$+6(-2A+\lambda+\lambda N)\mathrm{Re})\eta^3)$$
$$+\frac{1}{48}(2A\gamma_1 - \lambda(\gamma_1+\gamma_3+(\gamma_1+\gamma_7+\delta)N)$$
$$+\lambda(1+N)\mathrm{Re})\eta^4$$
$$-\frac{1}{240}(\lambda(\gamma_1+(\gamma_1+\delta)N))\eta^5]$$

Eqn. (A.1)

$$g(\eta) = (0) + p(0) + p^2[\frac{5}{48}\gamma_2(-2A+\lambda+\lambda N)$$
$$+\frac{7}{720}\gamma_2\lambda(1+N)\eta$$
$$+\frac{1}{8}\gamma_2(2A - \lambda(1+N))\eta^2 - \frac{1}{72}(\gamma_2\lambda(1+N))\eta^3$$
$$+\frac{1}{48}\gamma_2(-2A+\lambda+\lambda N)\eta^4$$
$$+\frac{1}{240}\gamma_2\lambda(1+N)\eta^5]$$

Eqn. (A.2)

$$\Theta(\eta) = \frac{1}{2}(1+\eta) + p[\frac{1}{4}(-\gamma_3+\gamma_3\eta^2)]$$
$$+p^2[\frac{1}{4}\gamma_6(\gamma_7+\delta)$$
$$+\frac{1}{12}(-\gamma_3^2+\gamma_6\delta)\eta) - \frac{1}{4}(\gamma_6(\gamma_7+\delta)\eta^2)$$
$$+\frac{1}{12}(\gamma_3^2 - \gamma_6\delta)\eta^3]$$

Eqn. (A.3)

$$\Phi(\eta) = \frac{1}{2}(1+\eta) + p[\frac{1}{4}(\gamma_7 - \delta) - \frac{1}{12}\delta\eta)$$
$$+\frac{1}{4}(\gamma_7+\delta)\eta^2 + \frac{1}{12}\delta\eta^3]$$
$$+p^2[\frac{1}{48}(12\gamma_3\gamma_8+\delta(6\gamma_7+5\delta))$$
$$+\frac{1}{720}(-60\gamma_7^2 - 60\gamma_7\delta + 7\delta^2)\eta$$

Eqn. (A.4)

Table 1. Hall Effects-Nusselt Number, Sherwood Number and Skin Friction Relation

M	$f'(-1)$	$-\Theta'(-1)$	$-\Phi'(-1)$	$f'(+1)$	$-\Theta'(+1)$	$-\Phi'(+1)$
0.5	0.050691	-0.864643	-0.409089	0.050691	-0.864643	-0.622153
1.0	0.050871	-0.864643	-0.409089	0.050871	-0.864643	-0.622153
2.5	0.050417	-0.864643	-0.409089	0.051417	-0.864643	-0.622153
4.0	0.050665	-0.864643	-0.409089	0.051683	-0.864643	-0.622153
5.5	0.051801	-0.864643	-0.409089	0.051801	-0.864643	-0.622153
7.0	0.051861	-0.864643	-0.409089	0.051861	-0.864643	-0.622153

Table 2. Chemical Reaction Rate-Nusselt Number, Sherwood Number, and Skin Friction Relation

δ	$f'(-1)$	$-\Theta'(-1)$	$-\Phi'(-1)$	$f'(+1)$	$-\Theta'(+1)$	$-\Phi'(+1)$
0.5	0.051531	-0.864643	-0.409089	0.051531	-0.864643	-0.622153
1.0	0.051575	-0.864643	-0.396689	0.051576	-0.863460	-0.654153
2.5	0.051708	-0.864643	-0.364156	0.051709	-0.859910	-0.744820
4.0	0.051842	-0.864643	-0.338623	0.051842	-0.856360	-0.827487
5.5	0.051975	-0.864643	-0.320089	0.051976	-0.852810	-0.902153
7.0	0.052108	-0.864643	-0.308556	0.052109	-0.849260	-0.968820